Dynamic arrest within the self-consistent generalized Langevin equation of colloid dynamics

L. Yeomans-Reyna,[1] M. A. Chávez-Rojo,[2] P. E. Ramírez-González,[3] R. Juárez-Maldonado,[3]
M. Chávez-Páez,[3] and M. Medina-Noyola[3]

[1]*Departamento de Física, Universidad de Sonora, Boulevard Luis Encinas y Rosales, 83000, Hermosillo, Sonora, México*

[2]*Facultad de Ciencias Químicas, Universidad Autónoma de Chihuahua, Venustiano Carranza S/N, 31000 Chihuahua, Chihuahua, México*

[3]*Instituto de Física "Manuel Sandoval Vallarta," Universidad Autónoma de San Luis Potosí, Álvaro Obregón 64, 78000 San Luis Potosí, SLP, México*

(Received 16 February 2007; revised manuscript received 26 July 2007; published 22 October 2007)

This paper presents a recently developed theory of colloid dynamics as an alternative approach to the description of phenomena of dynamic arrest in monodisperse colloidal systems. Such theory, referred to as the self-consistent generalized Langevin equation (SCGLE) theory, was devised to describe the tracer and collective diffusion properties of colloidal dispersions in the short- and intermediate-time regimes. Its self-consistent character, however, introduces a nonlinear dynamic feedback, leading to the prediction of dynamic arrest in these systems, similar to that exhibited by the well-established mode coupling theory of the ideal glass transition. The full numerical solution of this self-consistent theory provides in principle a route to the location of the fluid-glass transition in the space of macroscopic parameters of the system, given the interparticle forces (i.e., a nonequilibrium analog of the statistical-thermodynamic prediction of an equilibrium phase diagram). In this paper we focus on the derivation from the same self-consistent theory of the more straightforward route to the location of the fluid-glass transition boundary, consisting of the equation for the nonergodic parameters, whose nonzero values are the signature of the glass state. This allows us to decide if a system, at given macroscopic conditions, is in an ergodic or in a dynamically arrested state, given the microscopic interactions, which enter only through the static structure factor. We present a selection of results that illustrate the concrete application of our theory to model colloidal systems. This involves the comparison of the predictions of our theory with available experimental data for the nonergodic parameters of model dispersions with hard-sphere and with screened Coulomb interactions.

DOI: 10.1103/PhysRevE.76.041504 PACS number(s): 64.70.Pf, 61.20.Gy, 47.57.J−

I. INTRODUCTION

The dynamic properties of colloidal dispersions have been a subject of sustained interest for many years [1–3]. These properties can be described in terms of the relaxation of the fluctuations $\delta n(\mathbf{r},t)$ of the local concentration $n(\mathbf{r},t)$ of colloidal particles around its bulk equilibrium value n. The average decay of $\delta n(\mathbf{r},t)$ is described by the time-dependent correlation function $F(k,t)\equiv\langle\delta n(\mathbf{k},t)\delta n(-\mathbf{k},0)\rangle$ of the Fourier transform $\delta n(\mathbf{k},t)\equiv(1/N)\Sigma_{i=1}^{N}\exp[i\mathbf{k}\cdot\mathbf{r}_i(t)]$ of the fluctuations $\delta n(\mathbf{r},t)$, with $\mathbf{r}_i(t)$ being the position of particle i at time t. $F(k,t)$ is referred to as the intermediate scattering function, measured by experimental techniques such as dynamic light scattering. One can also define the *self*-component of $F(k,t)$, referred to as the self-intermediate scattering function, as $F_S(k,t)\equiv\langle\exp[i\mathbf{k}\cdot\Delta\mathbf{R}(t)]\rangle$, where $\Delta\mathbf{R}(t)$ is the displacement of any of the N particles over a time t.

In recent work a self-consistent theory of colloid dynamics has been developed [4–9], leading to the first-principles calculation of the dynamic properties above. This scheme allows the calculation of $F(k,t)$ and $F_S(k,t)$, given the effective interaction pair potential $u(r)$ between colloidal particles and the corresponding equilibrium static structure, represented by the radial distribution function $g(r)$ or the static structure factor $S(k)$. This theory, referred to as the self-consistent generalized Langevin equation (SCGLE) theory, is based on general and exact expressions [4] for $F(k,t)$ and $F_S(k,t)$ in terms of a hierarchy of memory functions, derived within the generalized Langevin equation (GLE) approach and the process of contraction of the description [10,11], and complemented by a number of physically or intuitively motivated approximations [5,6]. A systematic assessment of the intrinsic accuracy and limitations of the resulting approximate scheme under the simplest possible conditions (model monodisperse suspensions of spherical particles with no hydrodynamic interactions) has also been presented [7]. This was based on the comparison of the theoretical predictions for specific idealized model systems, with the corresponding Brownian dynamics computer simulation data in the short- and intermediate-time regimes. The same theoretical scheme has also been extended to describe the dynamics of colloidal mixtures [8,9]. The theoretical infrastructure just described is now being applied to study specific systems or phenomena. The main purpose of the present paper is to address the issue of its capability to describe the ideal ergodic-nonergodic transition in simple model colloidal systems.

The fundamental understanding of dynamically arrested states of matter is one of the most fascinating topics of condensed matter physics, and several issues related to their microscopic description are currently a matter of discussion [12–14]. Among the various approaches to the understanding of the transition from an ergodic to a dynamically arrested state, the mode coupling (MC) theory [14–17] provides perhaps the most comprehensive and coherent picture. In fact, a large number of experimental observations in specific sys-

tems, particularly in the domain of colloidal systems [18–22], seem to agree with the predictions of this theory.

The mode coupling theory of the ideal glass transition emerged originally in the framework of the dynamics of molecular (not colloidal) liquids [16,17]. Although one can expect [23] that the phenomenology of dynamic arrest does not depend on the short-time motion (which distinguishes between molecular and colloidal dynamics), it is convenient to base a theory for the glass transition of colloidal systems on the diffusive microscopic dynamics characteristic of these systems. In fact, in 1983 Hess and Klein [2] proposed the translation of the mode coupling self-consistent theory from the molecular context to colloidal systems, and extensive calculations based on such theory were eventually reported in the literature [24]. More recently, Nägele and collaborators developed a more elaborate version of this theory [25]. This scheme has been successfully extended and applied in several interesting directions [26], and the level of its quantitative accuracy at short and intermediate times has been documented [27,28], as well as its capability to predict the same scenario of dynamic arrest as the original MC theory (MCT).

The SCGLE theory that we shall discuss in this paper shares with the colloid-dynamics version of MCT developed by Nägele and collaborators [25] a number of important features. Most notably, both were developed with the intention to describe accurately the short- and intermediate-time dynamics of colloidal systems. They, however, differ radically in the conceptual framework upon which they are built. Thus, our theory is certainly not another version of MCT, and differs also from recent variants [29,30] of MCT mainly aimed at improving the performance of the original theory concerning the description of the ideal glass transition. Similarly, there is no direct relationship between the conceptual basis of the present theory and that of other theories of colloid dynamics partially or fully based on kinetic-theoretical concepts [31,32]. For this reason, one important aim of the present paper is to summarize the basic ingredients of the derivation of our theory.

The description of the transition to arrested states involves a large number of issues, which must be addressed systematically. One of the most crucial ones refers to the derivation of practicable, first-principles methods, to predict the location of the boundary between the ergodic and the arrested states of a system, given the effective forces between particles. In this paper we focus on this particular issue, which is the nonequilibrium analog of the statistical thermodynamic derivation of equilibrium phase diagrams. In principle, the set of coupled nonlinear dynamic equations that constitute the self-consistent theory must contain this information, and its numerical solution is the "brute force" but safer route to reveal it. In this paper, besides numerically solving the full self-consistent theory for the space and time dependence of all the dynamic properties involved, we focus on the derivation of a more direct criterion that allows us to locate the transition to dynamically arrested states in a much simpler manner.

This criterion consists of an equation for the nonergodic parameters, which are the long-time asymptotic values of the various dynamic properties involved, whose nonzero value is the signature of the glass state. Just as in MCT [14], this equation is derived from the long-time analysis of the self-consistent theory. In the present case, however, the resulting equations are reduced to a closed equation for a single scalar parameter, namely, the long-time value of the mean squared displacement of a tagged particle, that we denote as γ. This parameter has a finite value in the arrested state, and is infinite in the ergodic fluid state. Such an equation involves only the static structure factor $S(k)$ as an input. The solution of this equation allows then the determination of the wave-vector dependent collective nonergodic parameter $f(k)$ associated to the arrest of concentration fluctuations, which are written in a remarkably simple explicit expression that only involves $S(k)$ and γ.

We would like to stress that the main contribution of this paper is not some specific quantitative advantage of the theory presented, over MCT or other descriptions of dynamic arrest. Instead, the main contribution is the proposal of an alternative and independent perspective to model the glass transition. The expectation is that this alternative theoretical framework will join other approaches, most notably MCT, in the effort to improve our understanding and our predictive capability regarding dynamic arrest phenomena. We do expect, however, that the practical application of our self-consistent scheme will prove to be somewhat simpler than the use of MCT equations, and that this will facilitate its use by other people. For example, the extension of our theory to mixtures is rather straightforward, and this will allow its application to many specific systems and phenomena. In order to explain these advances, however, a preliminary step is to present the fundamental basis of our theory and to illustrate its application in the context of the simplest and most paradigmatic systems and phenomena; this is the main purpose of the present paper, which is explicitly limited to the context of monodisperse systems. Furthermore, in this paper we do not consider the effects of hydrodynamic interactions, which are fundamental in the discussion of the dynamic properties at short and intermediate times. As a working hypothesis, in this paper we shall assume that hydrodynamic interactions will not influence in a qualitative and fundamental manner the asymptotic long-time dynamics of the colloidal dispersion near its transition to dynamic arrested states nor the corresponding "phase diagram."

This paper is organized as follows. In the following section and in two appendixes we describe our self-consistent generalized Langevin equation (SCGLE) theory for colloid dynamics, and discuss very briefly the physical content and the rationale of each of the approximations involved in its formulation. In order for this paper to be reasonably self-contained, this will involve a certain degree of repetition with respect to Refs. [4–6,10], which contain all the details of its derivation and in which the quantitative accuracy of the most essential approximations of our theory is explicitly monitored. In Sec. III we derive the equations for the nonergodic parameters, and illustrate the manner in which this criterion is employed in the context of the hard-sphere system. In Sec. IV we present the numerical solutions of the full self-consistent theory for the time and wave-vector dependence of the intermediate scattering function of the same reference system. In Sec. V we present an illustrative selection of comparisons of the results of the present theory with

those measured in two experimental model systems. The first is the suspension of colloidal hard spheres, for which the transition is theoretically-predicted to occur at a volume fraction of $\phi_g=0.563$, in very close agreement with reported experimental results. The second is a colloidal suspension of charged particles. In Sec. VI we present particular details and limiting conditions concerning the Vineyard-like approximations introduced in this work. In Sec. VII we discuss and summarize our main results.

II. SELF-CONSISTENT GLE THEORY

The development of the self-consistent generalized Langevin equation theory involves four distinct fundamental elements [6]. The first consists of general and exact expressions for $F(k,z)$ and $F_S(k,z)$ [the Laplace transforms of $F(k,t)$ and $F_S(k,t)$, respectively], in terms of a hierarchy of memory functions. The second element consists of the formalization of the notion that collective dynamics should somehow be simply related to self-dynamics. This notion reduces the problem of colloid dynamics to the independent determination of $F_S(k,z)$ itself, or of its memory function $C_S(k,t)$. The third basic element of our theory is the proposal for the approximate determination of $C_S(k,t)$. This step is based on the physically intuitive expectation that space-dependent self-diffusion, represented by $F_S(k,t)$, should be simply related to the properties that characterize the Brownian motion of individual particles, such as the mean squared displacement. The fourth ingredient of the theory is provided by an independent expression for $\Delta\zeta(t)$, the time-dependent friction function that embodies the effects of interparticle interactions on the Brownian motion of individual tracer particles, and which can be approximately written in terms of $F(k,t)$ and $F_S(k,t)$, thus constituting a final closure of our fully self-consistent theory of colloid dynamics.

Let us now review each of these four elements in some more detail. In Ref. [4] the GLE approach and the concept of the contraction of the description [10,11] were employed to derive the most general time-evolution equation for the fluctuations $\delta n(\mathbf{r},t)$ of a monodisperse colloidal suspension in the absence of hydrodynamic interactions. In such derivation, the assumed underlying microscopic N-particle dynamics was provided by the many-particle Langevin equation [1]. As a result, expressions were derived for $F(k,t)$ and $F_S(k,t)$ [or their Laplace transforms $F(k,z)$ and $F_S(k,z)$] in terms of a hierarchy of memory functions, and of well-defined static structural properties of the Brownian fluid. In these expressions, the Brownian relaxation time $\tau_B \equiv M/\zeta^0$ (or the corresponding frequency $z_B \equiv \tau_B^{-1}$) appears, where M and ζ^0 are, respectively, the mass and the solvent-friction coefficient of each particle in the suspension. In the absence of friction ($\zeta^0 \to 0$), these expressions correspond to those of a simple atomic liquid [33,34]. In the presence of friction, and in order to "tune" these expressions to the time regime normally probed by dynamic light scattering experiments or by Brownian dynamics simulations, the limit $t \gg \tau_B$, or $z \ll z_B$, must be taken. Taking this so-called "overdamping" limit [4] requires a careful analysis, which was the main subject of Ref. [4]. As a result, one obtains the most general expression for $F(k,t)$ and $F_S(k,t)$ that describes the dynamics of the suspension in the diffusive regime (i.e., for times $t \gg \tau_B$). In Laplace space, the resulting "overdamped" expressions for $F(k,z)$ and $F_S(k,z)$ read [4]

$$F(k,z) = \frac{S(k)}{z + \dfrac{k^2 D_0 S^{-1}(k)}{1 + C(k,z)}} \tag{2.1}$$

and

$$F_S(k,z) = \frac{1}{z + \dfrac{k^2 D_0}{1 + C_S(k,z)}}, \tag{2.2}$$

where $C(k,z)$ and $C_S(k,z)$ are the respective memory functions.

We should mention that these results are exact, and can be derived in a variety of manners. They can be derived, for example, from the N-particle Smoluchowski dynamics using the projection operator formalism, $C(k,z)$ and $C_S(k,z)$ being referred to as the "irreducible memory functions" [25,26]. These general results constitute the starting point of the MCT, and they are also the basis of our present SCGLE theory. In our case, however, the generalized Langevin equation approach also provides exact expressions for the irreducible memory functions in terms of higher-order memory functions denoted by $\Delta L(k,z)$ and $\Delta L_S(k,z)$, namely,

$$C(k,z) = \frac{k^2 D_0 \chi^*(k)}{z + [\chi^*(k)]^{-1} L_0^*(k) + [\chi^*(k)]^{-1} \Delta L^*(k,z)} \tag{2.3}$$

and

$$C_S(k,z) = \frac{k^2 D_0 \chi_S^*(k)}{z + [\chi_S^*(k)]^{-1} L_{0S}^*(k) + [\chi_S^*(k)]^{-1} \Delta L_S^*(k,z)}. \tag{2.4}$$

In these equations, $D_0 = k_B T/\zeta^0$ is the free-diffusion coefficient of each particle ($k_B T$ being the thermal energy), $S(k)$ the static structure factor, and $\chi^*(k)$ the static correlation function of the fluctuations of the configurational component of the stress tensor of the Brownian fluid. $\chi^*(k)$ and $L_0^*(k)$, along with their self-counterparts $\chi_S^*(k)$ and $L_{0S}^*(k)$, are static properties, which can be written exactly [see Eqs. (A1)–(A3) of Appendix A] in terms of the two- and three-particle correlation functions, $g(r)$ and $g^{(3)}(\mathbf{r},\mathbf{r}')$, which are assumed to be known. In practice, the use of Kirkwood's superposition approximation allows us to write these properties in terms only of $g(r)$ [see Eq. (A6)]. Thus, the only unknown properties in the expressions for $F(k,t)$ and $F_S(k,t)$ in Eqs. (2.1)–(2.4) are the memory functions $\Delta L^*(k,z)$ and $\Delta L_S^*(k,z)$.

Neglecting $\Delta L^*(k,z)$ and $\Delta L_S^*(k,z)$ in Eqs. (2.3) and (2.4) leads to the so-called single exponential (SEXP) approximation [35,36], which consists of Eqs. (2.1) and (2.2) with

$$C(k,z) \approx C^{SEXP}(k,z) \equiv \frac{k^2 D_0 \chi^*(k)}{z + [\chi^*(k)]^{-1} L_0^*(k)} \tag{2.5}$$

and

$$C_S(k,z) \approx C_S^{SEXP}(k,z) \equiv \frac{k^2 D_0 \chi_S^*(k)}{z + [\chi_S^*(k)]^{-1} L_{0S}^*(k)}. \quad (2.6)$$

This approximation is exact at short times and/or large wave vectors, an important fact employed below.

As the second ingredient of the self-consistent theory, we search for a simple approximate relation between collective and self-dynamics. Vineyard's approximation [37], which relates $F(k,t)$ directly to $F_S(k,t)$ as $F(k,t) \approx F_S(k,t)S(k)$, is a simple (although qualitatively and quantitatively rather primitive [33,34]) implementation of this idea. Our proposal is, instead, to relate the memory function of $F(k,t)$ with the corresponding memory function of $F_S(k,t)$. In Ref. [5], a detailed numerical study of alternative such manners to refer collective dynamics to self-diffusion was carried out. Equations (2.1)–(2.4) suggest to relate $F(k,z)$ and $F_S(k,z)$ at the level of their highest-order memory functions. It was found, indeed, that a very accurate approximation was $\Delta L^*(k,z)/L_0(k) = \Delta L_S^*(k,z)/L_{0S}^*(k)$. In practice, however, it was also found [5] that equally precise connections could also be achieved at the level of the second-order memory functions $C(k,z)$ and $C_S(k,z)$. Two specific proposals of such Vineyard-like approximations were considered [6,9], which can be written in the generic form

$$C(k,z) = w(k,z)C_S(k,z) + y(k,z), \quad (2.7)$$

with $w(k,z)$ and $y(k,z)$ being known functions. The first approximates the ratio $C(k,z)/C_S(k,z)$ by its SEXP value,

$$C(k,z) = \left[\frac{C^{SEXP}(k,z)}{C_S^{SEXP}(k,z)}\right] C_S(k,z), \quad (2.8)$$

where the SEXP memory functions are given by Eqs. (2.5) and (2.6). This is referred to as the "multiplicative" Vineyard-like approximation, and corresponds to $w(k,z) = [C^{SEXP}(k,z)/C_S^{SEXP}(k,z)]$ and $y(k,z)=0$. The second approximates the difference $[C(k,z) - C_S(k,z)]$ by its SEXP value, and is referred to as the "additive" Vineyard-like approximation. It is defined by $w(k,z)=1$ and $y(k,z) = [C^{SEXP}(k,z) - C_S^{SEXP}(k,z)]$, i.e.,

$$C(k,z) = C_S(k,z) + [C^{SEXP}(k,z) - C_S^{SEXP}(k,z)]. \quad (2.9)$$

Later on we shall discuss the merits and deficiencies of these two specific proposals. Either of them, however, refer collective dynamics to self-dynamics, represented by the irreducible memory function $C_S(k,z)$. Thus, we must search for some form of approximation for this memory function.

The third ingredient of the present theory consists of the proposal for the approximate determination of $C_S(k,t)$. One intuitively expects that these properties should be simply related to the properties that describe the Brownian motion of individual particles, just like in the Gaussian approximation [1,2], which expresses $F_S(k,t)$ in terms of the mean squared displacement $W(t)$ as $F_S(k,t) = \exp[-k^2 W(t)]$. The present self-consistent theory introduces an analogous approximate connection between the functions $F_S(k,t)$ and $W(t)$, but at the level of their respective memory functions. The memory function of $W(t)$ is the so-called time-dependent friction function $\Delta\zeta(t)$. Although we do not have a physically transparent notion to guide us, we know, however, two exact limits that $C_S(k,t)$ must satisfy. Thus, for large wave vectors $C_S(k,t)$ is given exactly by $C_S^{SEXP}(k,t)$, whereas for small wave vectors $C_S(k,t)$ is given exactly by the time-dependent friction function $\Delta\zeta(t)$. This function, normalized by the solvent friction ζ_0, is essentially the memory function of the velocity autocorrelation function. In Ref. [6] it was proposed to interpolate $C_S(k,t)$ between these two exact limits by means of the following expression:

$$C_S(k,t) = C_S^{SEXP}(k,t) + [\Delta\zeta^*(t) - C_S^{SEXP}(k,t)]\lambda(k), \quad (2.10)$$

where $\Delta\zeta^*(t) \equiv \Delta\zeta(t)/\zeta_0$, and $\lambda(k)$ is a phenomenological interpolating function, such that $\lambda(k \to 0) \to 1$, and $\lambda(k \to \infty) \to 0$. The detailed functional form of this interpolating function will be described shortly.

The last ingredient of our theory is an expression for the time-dependent friction function $\Delta\zeta^*(t)$. For this property, a general and exact result has also been derived [10] within the framework of the GLE approach; the corresponding derivation is summarized in Appendix B. Such an exact result, however, can be simplified by means of well-defined approximations [10], also indicated in Appendix B, to read

$$\Delta\zeta^*(t) \equiv \frac{\Delta\zeta(t)}{\zeta_0} = \frac{D_0 n}{3(2\pi)^3} \int d\mathbf{k} \left[\frac{kh(k)}{1 + nh(k)}\right]^2 F(k,t)F_S(k,t), \quad (2.11)$$

where $h(k) = [S(k) - 1]/n$. This approximate expression for $\Delta\zeta^*(t)$ is one of the most important ingredients of the present theory. Let us mention that exactly the same expression was first introduced to the context of colloid dynamics by Hess and Klein [6], with arguments borrowed from mode coupling theory. As it is apparent from the derivation in Appendix B, our derivation follows a completely independent line of reasoning, and provides possible systematic manners to relax the approximations involved.

A closed system of equations results from all the arguments and approximations above, which can be summarized by the exact results in Eqs. (2.1) and (2.2), complemented with either of the Vineyard-like approximations of the generic form in Eq. (2.7), plus the interpolating formula in Eq. (2.10), along with the closure relation for the time-dependent friction function in Eq. (2.11). All the elements entering in these equations, including the SEXP approximation for the memory functions in Eqs. (2.5) and (2.6), involve only static properties, which can be determined by the methods of equilibrium statistical thermodynamics, given the potential $u(r)$ of the pairwise forces between the particles. Concerning the interpolating function $\lambda(k)$, a functional form of the general type $\lambda(k) = [1 + (k/k_c)^\nu]^{-1}$ was proposed [6], and the choice of the parameters k_c and ν was made by comparing the theoretical predictions for various values of k_c and ν with exact

(computer simulated) data for a particular model system, at a given state, and at a given time. This led to the following prescription for $\lambda(k)$,

$$\lambda(k) = \frac{1}{1 + \left(\frac{k}{k_{\min}}\right)^2}, \tag{2.12}$$

where $k_{\min}$ is the position of the first minimum of the static structure factor $S(k)$ of the system. This turns out to be an excellent interpolating device for all systems considered so far. Although no fundamental basis is available for this choice of $\lambda(k)$, this definition is universal (in the sense that it is the same for any system or state), and renders the resulting self-consistent scheme free from any form of adjustable parameters.

Since this self-consistent theory was not conceived within the theoretical framework of mode coupling theory (MCT), it makes little sense to define it in terms of a certain choice of the so-called vertex function, i.e., the specific manner in which the memory functions $C(k,z)$ and $C_S(k,z)$ are expressed in terms of $F(k,z)$ and $F_S(k,z)$ themselves. In our case, however, we may say that such a relation is contained in the (multiplicative or additive) Vineyard-like approximation, Eq. (2.7), plus the closure relation for $C_S(k,z)$ in terms of the time-dependent friction function in Eq. (2.10), along with the approximate expression in Eq. (2.11) for $\Delta\zeta^*(t)$ in terms of the intermediate scattering functions. We should mention that the general scenario of the ideal glass transition provided by our theory at this level of approximation, however, seems to be remarkably similar to that predicted by the MCT concerning, for example, the qualitative phenomenology of the relaxation of $F(k,t)$ and $F_S(k,t)$ near the transition, as illustrated below with the full solution of this self-consistent system of equations. Before that, however, let us discuss the prediction of the theory regarding the location of the boundary between ergodic and nonergodic states.

III. NONERGODIC PARAMETERS AND THE LOCATION OF THE GLASS TRANSITION

In this section we derive a criterion that allows us to locate the glass transition in a particularly simple manner, using only the static structure factor as an input. This criterion is the prediction of our theory concerning the long-time asymptotic value of the various dynamic properties. For the intermediate scattering function, $f(k) \equiv \lim_{t\to\infty} F(k,t)/S(k)$ is referred to as the nonergodic parameter. Here we also define $c(k) \equiv \lim_{t\to\infty} C(k,t)$, $c_S(k) \equiv \lim_{t\to\infty} C_S(k,t)$, and $\Delta\zeta^{*(\infty)} \equiv \lim_{t\to\infty} \Delta\zeta^*(t)$. The nonzero value of these nonergodic parameters is a signature of the glass state. The equation that determines $\Delta\zeta^{*(\infty)}$ constitutes the criterion referred to above.

To derive this criterion, let us substitute the dynamic properties above, involved in the self-consistent system of equations in Eqs. (2.1), (2.2), and (2.9)–(2.11), by the sum of their asymptotic long-time value plus the rest (which, by definition, always relaxes to zero). In the resulting system of equations, let us now take the asymptotic long-time limit, thus generating the following self-consistent system of equations for the "nonergodic" parameters of the properties involved:

$$f(k) = \frac{c(k)}{c(k) + k^2 D_0 S^{-1}(k)}, \tag{3.1}$$

$$f_S(k) = \frac{c_S(k)}{c_S(k) + k^2 D_0}, \tag{3.2}$$

$$c(k) = w(k) c_S(k), \tag{3.3}$$

$$c_S(k) = \lambda(k) \Delta\zeta^{*(\infty)}, \tag{3.4}$$

and

$$\Delta\zeta^{*(\infty)} = \frac{D_0 n}{3(2\pi)^3} \int d\mathbf{k} \frac{[kh(k)]^2}{1 + nh(k)} f(k) f_S(k), \tag{3.5}$$

with $w(k) \equiv w(k, z=0)$. Using Eqs. (3.3) and (3.4) in Eqs. (3.1) and (3.2), we can express the nonergodic parameters $f(k)$ and $f_S(k)$ in terms of $\Delta\zeta^{*(\infty)}$. Substituting the resulting expressions in Eq. (3.5), we finally obtain the following closed equation for $\Delta\zeta^{*(\infty)}$:

$$\Delta\zeta^{*(\infty)} = \frac{D_0 n}{3(2\pi)^3} \int d\mathbf{k} \frac{[kh(k)\lambda(k)\Delta\zeta^{*(\infty)}]^2 w(k)}{[1 + nh(k)][w(k)\lambda(k)\Delta\zeta^{*(\infty)} + k^2 D_0 S^{-1}(k)][\lambda(k)\Delta\zeta^{*(\infty)} + k^2 D_0]}. \tag{3.6}$$

Clearly, this equation always admits the trivial solution $\Delta\zeta^{*(\infty)} = 0$, which corresponds to the ergodic fluid state. The existence of other nonzero real solution(s) is associated to the glass state. The ideal glass transition is located at the boundary of the region where this equation ceases to have real solutions other than the trivial ergodic solution. In practice, we eliminate the trivial solution by dividing Eq. (3.6) by $\Delta\zeta^{*(\infty)}$, and rewriting it as

$$\Phi[\gamma; S] \equiv \frac{1}{6\pi^2 n} \int_0^\infty dk k^4 \frac{[S(k) - 1]^2 \lambda^2(k) w(k) \gamma}{[w(k)\lambda(k)S(k) + k^2\gamma][\lambda(k) + k^2\gamma]} = 1, \tag{3.7}$$

with γ defined as $\gamma \equiv D_0/\Delta\zeta^{*(\infty)}$. That γ is the mean squared displacement can be seen from the fact that if the time-dependent friction function $\Delta\zeta^*(t)$ decays to a nonzero value

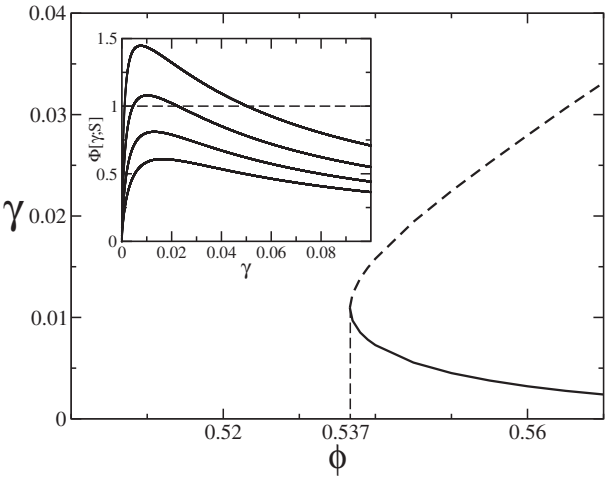

FIG. 1. Real solutions γ of Eq. (3.7) with $w(k)=1$. Below $\phi_g=0.537$ this equation has no real solutions. Above ϕ_g two solutions appear, illustrated by the two branches that bifurcate at ϕ_g. The branch for which γ decreases with ϕ (solid line) corresponds to the physical solution of the glass state. In the inset we plot the functional $\Phi[\gamma;S]$ as a function of γ for the volume fractions $\phi=0.45$, 0.50, 0.55, and 0.60 (from bottom to top).

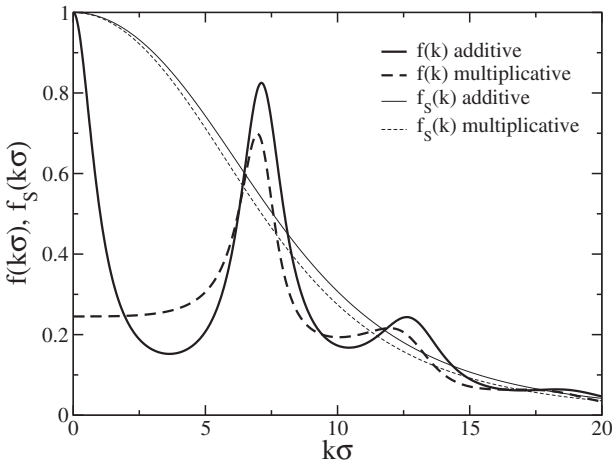

FIG. 2. Nonergodic parameters $f(k)$ (heavier solid line) and $f_S(k)$ (lighter solid line) calculated with Eqs. (3.8) and (3.9), respectively, with $w(k)=1$ (additive Vineyard-like approximation), for the HS system with $S(k)$ given by the PY approximation at the ideal glass transition volume fraction $\phi_g=0.537$. The dashed lines are the corresponding results for the multiplicative Vineyard-like approximation [$w(k)$ given by Eq. (3.10)], at its transition volume fraction $\phi_g=0.513$.

$\Delta\zeta^{*(\infty)}$, then this generates a harmonic force term in the effective Langevin equation that describes the Brownian motion of a representative tracer particle [see Eq. (B5) of Appendix B], with a spring constant given by $\zeta_0\Delta\zeta^{*(\infty)}$. From the equipartition theorem, it then follows that $\langle[\Delta x(t)]^2\rangle = k_BT/[\zeta_0\Delta\zeta^{*(\infty)}]=\gamma$.

In terms of γ, Eqs. (3.1) and (3.2) for the nonergodic parameters $f(k)$ and $f_S(k)$ read

$$f(k)=\frac{w(k)\lambda(k)S(k)}{w(k)\lambda(k)S(k)+k^2\gamma} \tag{3.8}$$

and

$$f_S(k)=\frac{\lambda(k)}{\lambda(k)+k^2\gamma}. \tag{3.9}$$

These equations clearly show that γ and the nonergodic parameters $f(k)$ and $f_S(k)$ only depend on the static structural properties $w(k)$, $\lambda(k)$, and $S(k)$, and not on transport properties, such as D_0. In Eq. (3.7), $\Phi[\gamma;S]$ is a functional of $S(k)$ and an ordinary function of γ. Thus, for a fixed state, i.e., for fixed $S(k)$, this equation may be solved by plotting $\Phi[\gamma;S]$ as a function of γ to see if it crosses unity, and for which value(s) of γ it does so. This procedure leads to the determination of the real nonzero solutions of Eq. (3.7).

This is illustrated in Fig. 1 for the hard-sphere (HS) system, using the static structure factor $S(k)$ given by the solution of the Percus-Yevick (PY) approximation [33,38] in the evaluation of the functional $\Phi[\gamma;S]$ with $w(k)=1$ (additive Vineyard-like approximation). Let us mention that later on in this paper we shall attempt a quantitative comparison of the theoretical predictions of our dynamical theory with experimental data. At that moment we will compare the additive with the multiplicative approximations, and will replace the PY by other more accurate approximations for $S(k)$. In this section, however, we base our illustrative calculations on the PY approximation, since its analytic solution [39] makes it very easy to program, so that anybody can reproduce the numbers reported here. Of course, the qualitative picture gained will not be affected by these quantitative details.

The inset of Fig. 1 exhibits the dependence of the functional $\Phi[\gamma;S]$ on γ for various volume fractions. Clearly, below a threshold volume fraction ϕ_g, $\Phi[\gamma;S]$ remains below 1 for all γ, and hence, there are no real solutions. Thus, the system must be in the ergodic state, described by the trivial solution with $\Delta\zeta^{*(\infty)}=0$ (i.e., $\gamma=\infty$). Above ϕ_g there are two real solutions, one of which corresponds to the glass state. In this manner, we determine this threshold value to be $\phi_g=0.537$, which is then the prediction of this criterion for the ideal glass transition volume fraction when the PY static inputs are employed. As indicated in Fig. 1, right at the transition there is only a single solution for γ, namely, $\gamma=1.094\times10^{-2}\sigma^2$, where σ is the hard-sphere diameter. This solution for γ may then be employed in Eqs. (3.8) and (3.9) to determine the nonergodic parameters $f(k)$ and $f_S(k)$; in Fig. 2 these properties are plotted for the HS system at its glass transition volume fraction.

For volume fractions beyond the transition, in the glass state, one must choose as the physical solution the branch corresponding to the smallest of the two mathematical nonzero solutions for γ (solid curve in Fig. 1). The reason for this is that one can show that γ is actually the mean squared displacement of the colloidal particles, as they rattle confined to the frozen cage formed by their neighbors. Since the size of this cage decreases with increasing volume fraction, the mean squared displacement γ should decrease as well.

The same calculations can be performed for the multiplicative Vineyard-like approximation. Let us mention, however, that in this case the function $w(k)\equiv C^{SEXP}(k,z=0)/$

$C_S^{SEXP}(k,z=0)$ contains integrals of derivatives of the pair potential involved in the second and third short-time moment conditions. These short-time moments do not exist for the hard-sphere potential (or for other discontinuous interactions), due to the divergence of such integrals; this reflects the nonanalytic behavior of $F(k,t)$ and its memory function at $t=0$ for these potentials [2,3]. It happens, however, that the divergent functions $C^{SEXP}(k,z=0)$ and $C_S^{SEXP}(k,z=0)$ above can be evaluated for a soft-sphere potential $u(r)\sim r^{-\nu}$, and the hard-sphere limit $\nu\to\infty$ limit can be taken in the result for their ratio $w(k)$. This leads to the finite limit

$$w^{HS}(y) = 1 - 3(y^2 \sin y + 2y \cos y - 2 \sin y)/y^3, \tag{3.10}$$

with $y=k\sigma$. This expression, along with the PY approximation for $S(k)$, allows us to apply Eqs. (3.7)–(3.9) above to the hard-spheres system, with the results $\gamma=1.27\times10^{-2}\sigma^2$ and $\phi_g=0.513$. The corresponding result for the non-ergodic factors are also displayed in Fig. 2.

IV. FULL SOLUTION OF THE SELF-CONSISTENT SCHEME

The criterion above constitutes a shortcut to the quick determination of the ergodic-nonergodic transition. An alternative lengthier route is the actual numerical solution of the full self-consistent set of equations in Eqs. (2.1), (2.2), and (2.5)–(2.12), as illustrated in this section. For this, Eqs. (2.1) and (2.2) are first Laplace inverted, and written as a set of coupled integrodifferential equations involving functions of k and t. These equations, complemented with Eqs. (2.5)–(2.12), are then discretized in a mesh of points large enough to ensure independence of the solution with respect to the size of the mesh. The discretized system of equations is solved by the method described in Refs. [40,41]. Previous to this procedure, one first has to determine the radial distribution function $g(r)$ for the desired pair potential, and then calculate the other static properties [$S(k)$, $\chi^*(k)$, $L_0^*(k)$, $\chi_S^*(k)$, and $L_{0S}^*(k)$].

There is, however, a little technicality to mention, concerning the application of the full self-consistent theory to the hard-sphere system, and has to do with the integrals that define the static properties $\chi^*(k)$, $L_0^*(k)$, $\chi_S^*(k)$, and $L_{0S}^*(k)$. As indicated above, these integrals involve derivatives of the pair potential, which do not exist for the hard-sphere system (the criterion derived in the previous section does not have this limitation, since it involves only the static structure factor as an input). We can circumvent this limitation, however, taking advantage of the principle of dynamic equivalence between soft and hard spheres explained in Ref. [42]. Thus, in order to apply the full theory to the HS system, one actually applies it to a soft-sphere system, and a simple rescaling of the results allows us to obtain the properties of the HS system. We have carried out this exercise within the PY approximation for $S(k)$ (which, for soft-sphere potentials, has to be solved numerically).

Proceeding in this manner, at any arbitrary state, we can calculate all the dynamic properties, including $F(k,t)$, $F_S(k,t)$, and $\Delta\zeta(t)$, and check directly if these properties decay to zero or not, thus leading to the prediction of the location of the glass transition, and of the values of the nonergodic parameters at the transition, and in general, at other glass states. Of course, the results thus obtained turn out to coincide exactly with those of the static criterion above (Sec. III). For example, for the hard-sphere system within the Percus-Yevick approximation this procedure leads, in the case of the additive Vineyard-like approximation, to the location of the glass transition at $\phi_g=0.537$, and to the same value of the nonergodic parameter $\Delta\zeta^{*(\infty)}$ determined in Sec. III ($\gamma=D_0/\Delta\zeta^{*(\infty)}=1.094\times10^{-2}\sigma^2$). Finally, the nonergodic parameters $f(k)$ and $f_S(k)$ determined by this exact route agree with those determined in Sec. III (plotted as the solid curves in Fig. 2). Similar comments apply in the case of the multiplicative Vineyard-like approximation.

Let us now discuss the relevance of the accuracy of the static structural properties [$S(k)$ and $g(r)$] employed as inputs in the actual applications of the self-consistent dynamic theory. As indicated before, all the illustrative numerical calculations reported so far have referred to the hard-sphere system, and have involved, for simplicity, the use of the Percus-Yevick approximation for the input static properties $S(k)$ and $g(r)$. The use of this approximation is itself a source of inaccuracies, which we can minimize or eliminate. For the HS system, we improve the PY approximation with the semiempirical Verlet-Weis (VW) modification [43], which provides virtually exact hard-sphere radial distribution functions up to the freezing transition.

The first noticeable consequence of improving the input static properties is a rather dramatic change in the prediction of the location of the ideal glass transition, from $\phi_g=0.537$ with the PY approximation, to $\phi_g=0.563$ with the Verlet-Weis-improved Percus-Yevick (PY-VW) approximation. The mean squared displacement parameter γ changes from $\gamma=1.094\times10^{-2}\sigma^2$ to $\gamma=1.060\times10^{-2}\sigma^2$. The corresponding change in the nonergodic parameters $f(k)$ and $f_S(k)$ turns out to be rather insignificant, and the new results virtually superimpose on the solid lines of Fig. 2. Similar observations apply for the multiplicative Vineyard-like approximation, with ϕ_g increasing from its PY value $\phi_g=0.513$ to $\phi_g=0.537$, and with γ decreasing from $\gamma=1.27\times10^{-2}\sigma^2$ to $\gamma=1.23\times10^{-2}\sigma^2$. From now on in this paper, when referring to the results of our theory for the hard-sphere system, we shall refer to the results obtained with the more accurate PY-VW approximation for the static properties.

The numerical solution of the self-consistent theory provides the complete scenario of the relaxation of the dynamics of the system, and of the process of dynamic arrest, as the glass transition is approached. Here we illustrate this process with the theoretical results for the relaxation of the intermediate scattering function described by our theory within the additive approximation in the vicinity of the hard-sphere glass transition. In Fig. 3 we plot the correlator $f(k,t)\equiv F(k,t)/S(k)$ as a function of time (in units of $t_0\equiv\sigma^2/D_0$) at hard-sphere volume fractions $\phi=0.559$, 0.560, 0.561, 0.562, and $0.563(=\phi_g)$, with the input static properties provided by the PY-VW approximation. In reality, the short-time dynamics of our theory requires static information that is not de-

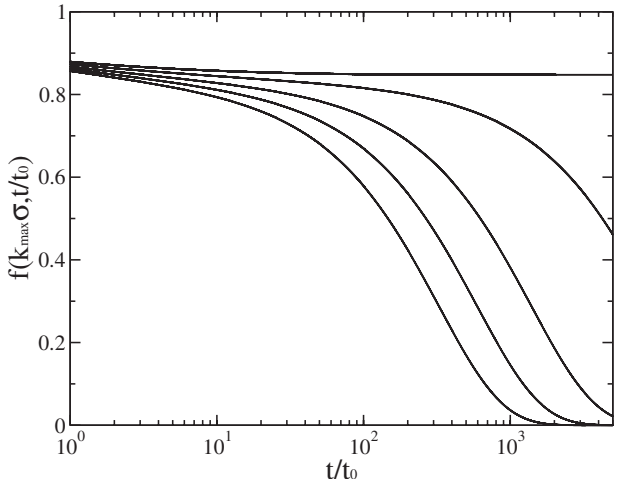

FIG. 3. Time-relaxation of the collective correlator $f(k,t) \equiv F(k,t)/S(k)$ for the HS system in the vicinity of the glass transition, for the hard-sphere volume fractions (from bottom to top) $\phi = 0.559$, 0.560, 0.561, 0.562, and $0.563(=\phi_g)$. The time is expressed in units of $t_0 \equiv \sigma^2/D_0$.

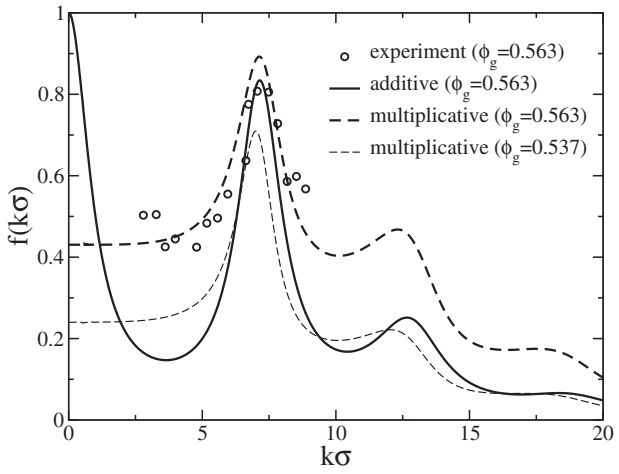

FIG. 4. Nonergodic parameter $f(k)$ calculated with Eqs. (3.7) and (3.8) within the additive (solid line) and the multiplicative (dashed lines) Vineyard-like approximations, for the HS system with $S(k)$ given by the PY-VW approximation, at the ideal glass transition volume fraction (solid and heavy lines for $\phi_g = 0.563$, light dashed line for $\phi_g = 0.537$). The circles are the experimental data of Ref. [19], measured at $\phi_g = 0.563$.

fined for the hard-sphere potential. As explained in detail in Ref. [42], however, the hard-sphere static and dynamic properties can be calculated for a dynamically equivalent soft-sphere system. Thus, our dynamic calculations for the HS system were in fact performed on a soft-sphere system with pair potential given, in units of the thermal energy $k_B T = \beta^{-1}$, by

$$\beta u_s(r) = \frac{1}{(r/\sigma_s)^{2\nu}} - \frac{2}{(r/\sigma_s)^{\nu}} + 1, \tag{4.1}$$

for $0 < r < \sigma_s$, and such that it vanishes for $r > \sigma_s$. The static input $S(k)$ for this system with $\nu = 100$ was provided by the method explained by Verlet and Weis [43], based of the solution of the Percus-Yevick approximation [38,39]. Thus, the curves in Fig. 3, corresponding to the sequence of hard-sphere volume fractions given above, also correspond to the ($\nu = 100$) soft-sphere volume fractions $\phi^{(s)} = 0.571$, 0.572, 0.573, 0.574, and $0.575(=\phi_g^{(s)})$, respectively. These two sets of volume fractions are related to each other through a simple rescaling, as explained in Ref. [42].

V. COMPARISON WITH EXPERIMENTAL DATA

Of course, the systematic and extensive comparison of the present theoretical predictions with the corresponding experimental or computer-simulated data is needed, and will be the subject of separate communications. Here, however, we present a selection of illustrative results, restricted to the analysis of the collective nonergodic parameter $f(k)$, for two systems for which experimental data are available, namely, the hard-sphere suspension and a suspension of highly charged particles at low ionic strength.

We first discuss the results for the hard-sphere system. The first noticeable theoretical prediction is the location of the ideal glass transition. The transition volume fraction predicted by our theory within the additive Vineyard-like approximation, $\phi_g = 0.563$, turns out to be in excellent agreement with the experimental results reported in Ref. [19]. At this volume fraction we found $\gamma = 1.060 \times 10^{-2}\sigma$. This leads to a ratio $\delta \equiv \sqrt{\langle [\Delta x(t)]^2 \rangle}/d$ of the localization length $\sqrt{\langle [\Delta x(t)]^2 \rangle} = \gamma^{1/2}$ to the mean interparticle distance $d \equiv n^{-1/3}$ of 0.105, strongly reminiscent of the Lindemann criterion of melting [46]. In contrast, the multiplicative Vineyard-like approximation leads to $\phi_g = 0.537$, sensibly smaller than the experimental value, and to a value of the Lindemann ratio of $\delta = 0.112$.

The other important property that we can compare to experimental data is the collective nonergodic parameter $f(k)$. In Fig. 4 we compare the theoretical results for $f(k)$ obtained from Eqs. (3.8) and (3.7) within the additive Vineyard-like approximation (solid line; input static properties provided by the PY-VW approximation) at the volume fraction $\phi_g = 0.563$, with the corresponding experimental data, also reported at $\phi_g = 0.563$ [19]. As we can see, the comparison is very good concerning the height and position of the first maximum of $f(k)$. We mention that the position of this maximum of $f(k)$ also coincides with the position of the main peak of the static structure factor (not shown in Fig. 4). We observe, however, that at smaller and larger wave vectors, the agreement between theory and experiment for $f(k)$ deteriorates appreciably.

On the other hand, in Fig. 4 we also plot the theoretical results obtained with the multiplicative Vineyard-like approximation (dashed lines), also using the PY-VW static structure factor $S(k)$. In one case (heavy dashed line), we employed the same input $S(k)$ as in the additive approximation (solid line), i.e., the PY-VW $S(k)$ at the actual experimental volume fraction $\phi_g = 0.563$. The light dashed line was obtained employing the PY-VW $S(k)$ at $\phi_g = 0.537$, which is the transition volume fraction predicted by the multiplicative approximation; thus, it corresponds to a zero separation pa-

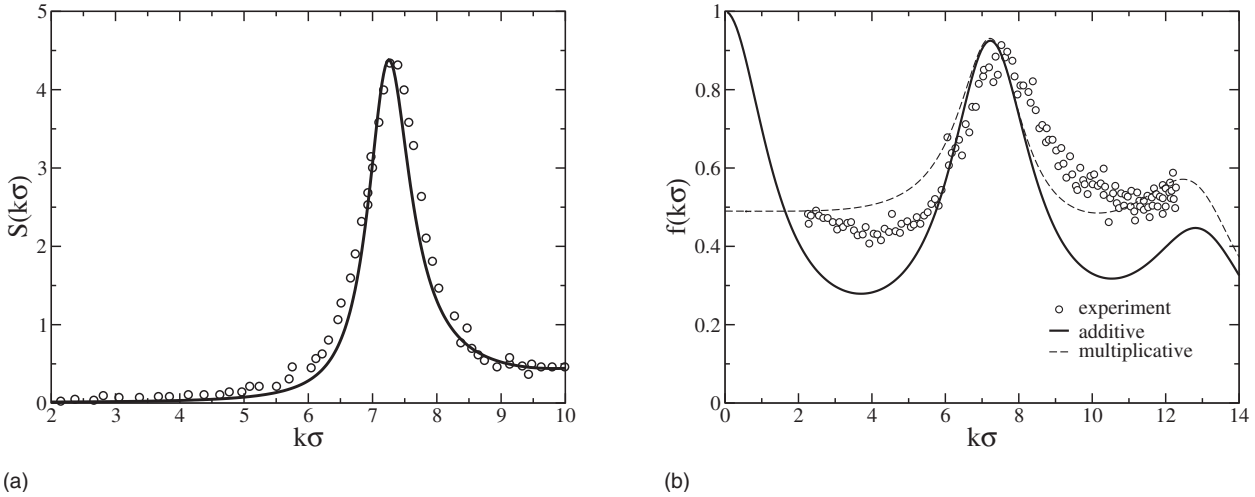

FIG. 5. (a) Static structure factor calculated with the PY-VW approximation (solid curve) for the HS system at volume fraction $\phi=0.58$; the symbols correspond to the experimental data of Ref. [22]. (b) Theoretical predictions for the nonergodic parameter $f(k)$ of a HS suspension at $\phi=0.58$ within the additive (solid line) and multiplicative (dashed line) Vineyard-like approximations; symbols correspond to experimental data reported in Ref. [22].

rameter $\eta \equiv (\phi-\phi_g)/\phi_g$ from the transition volume fraction $\phi_g=0.537$ predicted by this approximation. Clearly, the latter curve lies far below the experimental data, whereas the other two curves, in which the $S(k)$ at the experimentally determined volume fraction $\phi_g=0.563$ was employed, lie closer to the experimental data for $f(k)$. The latter calculation within the multiplicative approximation seems to have a similar degree of accuracy as the additive approximation with the same static input, although it overestimates the height of the main peak of $f(k)$. We must bear in mind, however, that these theoretical results of the multiplicative approximation correspond to a separation distance $\eta=0.05$. The results of the additive approximation, on the other hand, correspond to a null separation parameter, thus agreeing with the experimental data in this regard. Let us also notice an important qualitative difference between the additive and the multiplicative approximations, namely, their predictions for the long-wavelength limit of $f(k)$. As it was quite apparent already from the illustrative results in Fig. 2, the additive approximation leads to the limit $\lim_{k\to 0} f(k)=1$, whereas the multiplicative approximation leads to $\lim_{k\to 0} f(k)<1$. The meaning and relevance of this issue will be discussed below.

The nonergodic parameters can also be measured and calculated at volume fractions larger than ϕ_g, i.e., well inside the glass region. For example, Ref. [22] reports experimental data for the static structure factor and the nonergodic parameter of a hard-sphere system at a volume fraction $\phi=0.58$. Figure 5(a) shows the static structure factor calculated from the PY-VW approximation for this volume fraction; the experimental data of Ref. [22] are also included as a reference. This $S(k)$ was employed as the input of the dynamic theory in the calculation of the nonergodic parameter $f(k)$, and Fig. 5(b) illustrates the comparison of our theoretical predictions within both, the additive and the multiplicative approximations, with the corresponding experimental data. We find a similar scenario as observed in Fig. 4, except that now both theoretical predictions coincide in the height of the maximum of the nonergodic parameter, which is located at the position as the main peak of $S(k)$, whereas the position of the experimental first maximum of $f(k)$ is shifted to slightly larger wave vectors.

Let us finally illustrate the applicability of our theory to an additional system, this time representative of a colloidal system with softer interactions. We refer to a colloidal dispersion of charged particles, also reported in Ref. [22], whose effective pair potential may be modeled by the repulsive screened Coulomb potential,

$$\beta u(r) = \begin{cases} K\dfrac{\exp[-z(r/\sigma-1)]}{(r/\sigma)}, & r>\sigma; \\ \infty, & r<\sigma. \end{cases} \tag{5.1}$$

This corresponds to the electrostatic contribution of the well-known Derjaguin-Landau-Verwey-Overbeek (DLVO) potential [44,45], in which the interaction parameters z and K are, respectively, the inverse Debye screening length (in units of σ), and the intensity of the pair potential at hard-sphere contact (in units of k_BT). Experimental data for this system are also reported in Ref. [22]. For one of the samples, the hard-sphere diameter and the volume fraction ϕ are experimentally determined to be $\sigma=272$ nm and $\phi=0.27$, and data are provided for the static structure factor. In order to use these data as the static input in the dynamic theory, we need to have a smooth representation of the experimental data for $S(k)$, and hence, we had to fit these data. For this we used, as a fitting device, the static structure factor calculated within the hypernetted chain (HNC) approximation [33] for the potential above, and the solid line in Fig. 6(a) corresponds to the best fit, with $z=3.1587$ and $K=11.6555$. This fit was actually made not by varying z and K independently, but by using the expressions for these parameters in terms of the charge $Q=Ze^-$ of the particles provided by the DLVO model [3,45], namely, $z=\sqrt{24\phi Z l_B/\sigma}$ and $K=l_BZ^2/[\sigma(1+z/2)^2]$,

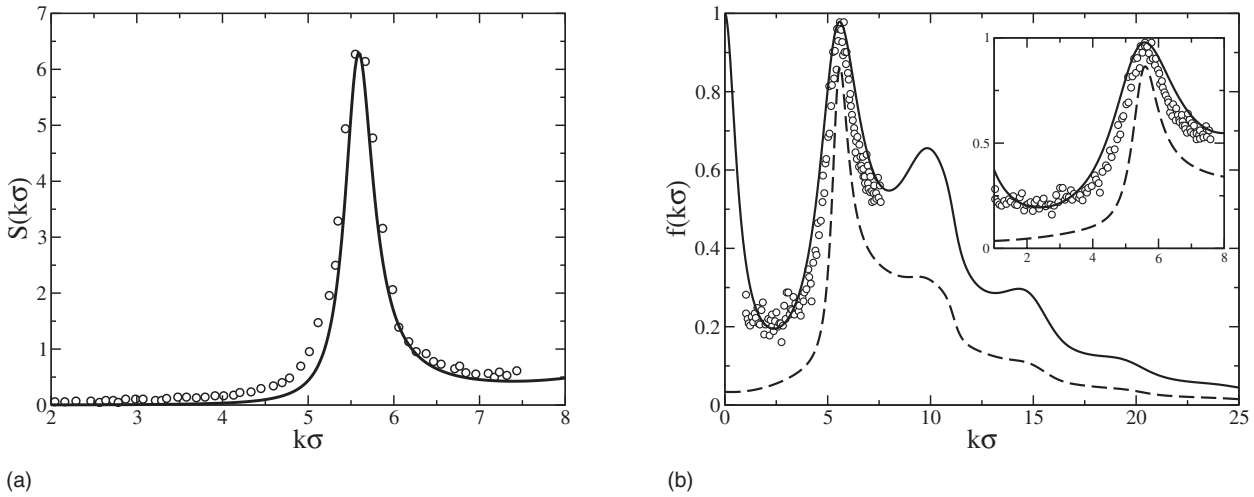

FIG. 6. (a) Static structure factor calculated with the HNC approximation, and (b) theoretical predictions for the nonergodic parameter $f(k)$ for the charged sphere system, with pairwise forces given by Eq. (5.1) at $\phi=0.27$, $z=3.1587$, and $K=11.6555$; symbols correspond to experimental data in Ref. [22], solid and dashed lines correspond to the additive and multiplicative Vineyard-like approximations, respectively. The inset in (b) enlarges the region where experimental data for $f(k)$ are available.

where $l_B=(e^-)^2/\epsilon k_B T$ is the Bjerrum length, and ϵ the dielectric constant of the solvent.

Next, we employed this $S(k)$ as the static input of the dynamic theory to calculate the nonergodic parameters, according to the general results in Sec. III. For this, we first calculated the mean squared displacement γ as the solution of Eq. (3.7), with the result $\gamma=2.85\times10^{-3}\sigma^2$ for the additive approximation, and $\gamma=8.68\times10^{-3}\sigma^2$ for the multiplicative approximation. The corresponding results for $f(k)$ are compared with the experimental data in Fig. 6(b). As we can see from this comparison, the agreement with the experimental data for the nonergodic parameter $f(k)$ of our theoretical predictions within the additive approximation turns out to be very good for all the wave vectors reported in the experiment, whereas the predictions of the multiplicative version turn out to be quantitatively less accurate.

VI. ADDITIVE VS MULTIPLICATIVE VINEYARD-LIKE APPROXIMATIONS

There is a number of issues regarding the advantages and limitations of the present SCGLE theory as a proposal of a competitive quantitative theory of dynamic arrest. Its detailed discussion falls outside the scope of the present introductory paper. Let us highlight, however, one particular salient feature, namely, the behavior of the nonergodic parameters in the small wave-vector limit predicted by Eqs. (3.8) and (3.9). Let us first notice that these two equations correctly predict that both $f(k)$ and $f_S(k)$ are smaller than unity for all *finite* wave-vectors k, as expected from general considerations [14]. From Eq. (3.9), however, we have that $\lim_{k\to0} f_S(k)=1$, and this holds for both the additive and the multiplicative approximations. On the other hand, Eq. (3.8) indicates that the collective nonergodic parameter $f(k)$ does depend explicitly on $w(k)$, and hence, these two versions of the SCGLE theory will differ in their predictions for $f(k)$, as illustrated in the previous section. Although both versions correctly predict that $f(k)<1$ for $k\neq0$, their long-wavelength description of $f(k)$ is qualitatively different. Thus, while the additive approximation predicts that $\lim_{k\to0} f(k)=1$, the multiplicative approximation predicts that $\lim_{k\to0} f(k)<1$; the latter can be seen by noticing that in general the function $w(k)\equiv C^{SEXP}(k,z=0)/C_S^{SEXP}(k,z=0)$ vanishes as k^2 for small k. This contrast between the additive and the multiplicative approximations is clearly apparent in Figs. 4–6. Unfortunately nobody has rigorously derived any form of "sum rule" that fixes the exact value of $f(0)$.

Let us mention that MCT predicts that $f_S(0)=1$ and that $f(0)<1$ [14], just the same as the multiplicative version of our SCGLE theory. The value $f(0)=1$ obtained from the additive SCGLE theory, on the other hand, represents an interesting physical concept, namely, that of a macroscopically infinitely rigid solid. The mechanical rigidity of a system can be described by its mechanical susceptibility $\tilde{\chi}(k)$, which can be written as $\tilde{\chi}(k)=[1-f(k)]\chi^T(k)$, where $\chi^T(k)$ is its thermodynamic susceptibility [proportional to $S(k)$] [33,34]. A fluid $[f(k)=0]$ may have zero mechanical susceptibility only when $\chi^T(k)$ vanishes; this would be the case of an incompressible fluid. In a glass, the condition $f(k)\approx1$ is referred to as the stiff glass approximation [48]. In this approximation, the glass is stiff $\{\tilde{\chi}(k)=[1-f(k)]\chi^T(k)\approx0\}$ because it is a rigid solid $\{[1-f(k)]\approx0\}$, and not because it is incompressible $[\chi^T(k)\approx0]$. We may have this condition to apply exactly only at $k=0$ $[f(0)=1$ but $f(k)<1$ for $k\neq0]$, and this defines an ideally stiff glass only at long wavelengths. Of course, such a condition is not met exactly by real systems [just as no real system behaves exactly as an ideal gas or as a hard-sphere fluid], but it defines a distinct and conceptually important reference state. The issue of how relevant this reference state may be to specific real systems must, of course, be submitted to experimental test [bearing in mind, in analyzing data pertaining to atomic glasses [49,50], possible fundamental differences between colloidal (strongly overdamped) and atomic (solvent-free) systems].

This issue is, of course, intimately related with our need to discriminate between the additive and the multiplicative approximations, concerning their qualitative, quantitative, and practical usefulness to describe the transition to dynamically arrested states. Nevertheless, in order to check the practical relevance of these qualitative differences between the additive and the multiplicative approximations, the predictions of the self-consistent theory, complemented in one case with the multiplicative and in the other with the additive Vineyard-like approximation, have been compared with the results of Brownian dynamics simulations for specific model systems [9]. From such comparisons, it was concluded that the difference of the predictions of both versions of the SCGLE theory are not quantitatively relevant, even in the regimes where these short-time conditions might be most important.

The issues just discussed do not provide a definitive criterion for discriminating between the additive and the multiplicative approximations. Thus, we must turn to the comparison of their specific predictions with the corresponding experimental measurements, as a more reliable criterion to prefer one or the other. Although the comparisons presented in the previous section must be complemented with additional similar tests, it seems to us pretty apparent that the additive SCGLE theory provides systematically better agreement with experiment. In addition, it provides a simpler description of the asymptotic long-time singular behavior, typical of the approach to dynamically arrested states. A practical bonus is that it also provides a considerable simplification of the application of the theory to the problem of locating the glass transition, since the corresponding criterion, namely, Eq. (3.7), only involves the static structure factor and not other static properties associated with the short-time moment conditions. For these reasons, and because the quantitative predictions are close enough to the experimental data to allow a direct comparison without the need of adjustable parameters or any form of rescaling of the volume fraction, we propose to adopt the additive Vineyard-like approximation in the SCGLE theory presented in this paper in future applications.

VII. SUMMARY AND DISCUSSION

In summary, in this paper we have introduced the self-consistent generalized Langevin equation theory of colloid dynamics as a practicable approach to the description of the phenomena of dynamic arrest in monodisperse colloidal systems. For this, we provided a summary of the main arguments, derivations, and approximations that serve as the basis in the construction of this self-consistent theory. We then focused on the problem of locating the boundary between the ergodic and nonergodic regions, and discussed an approach to achieve this, derived from the same self-consistent theory. This criterion, which in the MCT literature is referred to as the bifurcation equation, describes the condition needed to restore the ergodicity of the system when it approaches the fluid-glass boundary from the glass side. It consists of an equation for the nonergodic parameter, and the borderline condition is the failure of this equation to have nonzero solutions. This criterion only requires as an input the static structure factor of the system (which only depends on the interparticle interactions), and provides a shortcut to the goal of determining the fluid-glass boundary, alternative to the solution of the self-consistent set of equations describing the full time- and wave-vector-dependence of all the dynamic properties of the system.

One of the elements of the SCGLE theory, namely, the Vineyard-like connection between collective and self-dynamics, was the subject of special attention. We considered two versions of this connection, referred to as the additive and the multiplicative Vineyard-like approximations. Although at the end we endorse the former as the most accurate and useful one, we presented and contrasted the results of both approximations in their comparison with the experimental data. Before that, however, and as an illustration and initial calibration, we applied our theory to the hard-sphere system, first within the Percus-Yevick approximation for its static properties, yielding $\phi_g=0.537$, and then with the virtually exact Verlet-Weis-Percus-Yevick $S(k)$ (from now on, we only refer to the results of the additive approximation). In this manner we arrived at our prediction for the location of the glass transition of the hard-sphere system, $\phi_g=0.563$, which is about the best quantitative theoretical estimate of the location of the glass transition of the hard-sphere system. The comparison of the predicted nonergodic parameters at, and above, this glass transition volume fraction, with the corresponding experimental data, was presented in Figs. 4 and 5, respectively. These comparisons indicate that, for the volume fraction corresponding to ϕ_g, the agreement of the theory with the experimental data is very good regarding the height and position of $f(k)$ at its first maximum. A similar scenario was observed at the larger volume fraction, $\phi=0.58$, except that now we observe that the theoretical predictions place the maximum of $f(k)$ at the same position of the main peak of $S(k)$, whereas the experimental data for $f(k)$ exhibits this first maximum at slightly larger wave vectors. In contrast, the comparison in Fig. 6(b) with the experimental data of Ref. [22] for the nonergodic parameter of the dispersion of charged particles exhibits a remarkable qualitative and quantitative agreement. In particular, the position of the first maximum of $f(k)$ coincides with the position of the main peak of $S(k)$ according to both theory and experiment. We must stress that our theoretical predictions do not involve any sort of adjustable parameters.

As indicated in Sec. III, the parameter γ, solution of Eq. (3.7), is the mean squared displacement $\langle[\Delta x(t)]^2\rangle$ of the colloidal particles in the glass state, as they undergo Brownian motion inside the frozen cage formed by their neighbors. It is then interesting to find out if this quantity has any special value at the glass transition. According to the theoretical prediction for γ reported in the previous sections, the hard-sphere glass melts when $\gamma=1.060\times10^{-2}\sigma^2$, which means that the root mean square displacement is of the order of one tenth of the hard-sphere diameter; notice that at the volume fraction involved, $\phi_g=0.563$, the mean interparticle distance $d\equiv n^{-1/3}$ is $d=0.98\sigma$, so that $\delta=\sqrt{\langle[\Delta x(t)]^2\rangle}/d\approx0.105$. This is strongly reminiscent of the Lindemann criterion for the melting of a crystal [46]. A similar calculation for the

charged sphere suspension leads to similar conclusions. In fact, we find more generally that our theory predicts a very distinctive and universal Lindemann-like criterion for the melting of a glass for systems with repulsive (soft or hard) interactions. This, and many other issues related to the description of dynamic arrest in monodisperse suspensions, can be addressed with the present theory, which may also be extended to consider more complex and interesting situations. These issues, however, will be discussed in detail in future communications.

ACKNOWLEDGMENTS

This work was supported by the Consejo Nacional de Ciencia y Tecnología (CONACYT, México), through Grants No. SEP-2004-C01-47611 and No. SEP-2003-C02-44744, and of FAI-UASLP. The authors are deeply indebted to Professor J. Bergenholtz, Professor A. Banchio, and Professor G. Nägele for useful discussions. We are also particularly grateful to one of the anonymous referees for his and/or her exceptionally careful and critical reading of our manuscript.

APPENDIX A: STATIC PROPERTIES

For immediate reference, in this appendix we quote the expressions for the static properties $\chi^*(k)$, $L_{0S}^*(k)$, $\chi_S^*(k)$, and $L_{0S}^*(k)$ associated to $F(k,z)$ and $F_S(k,z)$ [see Eqs. (2.3) and (2.4)] in terms of the two- and three-particle correlation functions, $g(r)$ and $g^{(3)}(\mathbf{r},\mathbf{r}')$. For the details of their derivation, we refer the reader to the original source, namely, Ref. [6]. These expressions are

$$\chi^*(k) = 1 + n\int d^3r g(r)\frac{\partial^2 \beta u(r)}{\partial z^2}\left(\frac{1-\cos(kz)}{k^2}\right) - \frac{1}{S(k)}, \tag{A1}$$

$$\begin{aligned} L_0^*(k) = {} & nD_0\int d^3r g(r)\frac{\partial^2 \beta u(r)}{\partial z^2}[1+2\cos kz] - \frac{D_0 n^2}{k^2}\left[\int d^3r g(r)\frac{\partial^2 \beta u(r)}{\partial z^2}(1-\cos kz)\right]^2 \\ & + \frac{2D_0 n}{k}\int d^3r g(r)\frac{\partial^3 \beta u(r)}{\partial z^3}\sin kz + \frac{2D_0 n}{k^2}\int d^3r g(r)(1-\cos kz)\left[\frac{\partial \boldsymbol{\nabla}\,\beta u(r)}{\partial z}\right]^2 \\ & + \frac{D_0 n^2}{k^2}\int d^3r d^3r' g^{(3)}(\mathbf{r},\mathbf{r}')(1-2\cos kz+\cos[k(z-z')])\times\left[\frac{\partial \boldsymbol{\nabla}\,\beta u(r)}{\partial z}\right]\cdot\left[\frac{\partial \boldsymbol{\nabla}'\beta u(r')}{\partial z'}\right], \end{aligned} \tag{A2}$$

$$\chi_S^*(k) = \frac{1}{k^2}\left[n\int d^3r g(r)\frac{\partial^2 \beta u(r)}{\partial z^2}\right], \tag{A3}$$

and

$$\begin{aligned} k^2 L_{0S}^*(k) = {} & k^2 D_0\left[n\int d^3r g(r)\frac{\partial^2 \beta u(r)}{\partial z^2}\right] - D_0 n^2\left[\int d^3r g(r)\frac{\partial^2 \beta u(r)}{\partial z^2}\right]^2 + 2D_0 n\int d^3r g(r)\left[\frac{\partial \nabla\,\beta u(r)}{\partial z}\right]^2 \\ & + D_0 n^2\int d^3r d^3r' g^{(3)}(\mathbf{r},\mathbf{r}')\left[\frac{\partial \nabla\,\beta u(r)}{\partial z}\right]\cdot\left[\frac{\partial \nabla'\beta u(r')}{\partial z'}\right]. \end{aligned} \tag{A4}$$

In the equations above, $u(r)$ is the effective interaction pair potential between colloidal particles. Finally, we should mention that in this paper we have systematically dropped the subindex "UU" employed in Ref. [6], where $(k_BT/M)^2$ times $\chi^*(k)$, $\chi_S^*(k)$, $L_0^*(k)$, and $L_{0S}^*(k)$ are denoted, respectively, by $\chi_{UU}(k)$, $\chi_{UU}^{(S)}(k)$, $L_{UU}(k)$, and $L_{UU}^{(S)}(k)$.

The integrals involving $g^{(3)}(\mathbf{r},\mathbf{r}')$ in these equations were evaluated in practice with the use of Kirkwood's superposition approximation, $g^{(3)}(\mathbf{r},\mathbf{r}')\approx g(r)g(r')g(|\mathbf{r}-\mathbf{r}'|)$, plus the additional simplification of approximating $g(|\mathbf{r}-\mathbf{r}'|)$ by its asymptotic value of 1. This leads, in particular, to replacing the integral in the last term of Eq. (A2),

$$\Delta m^{(3)}(k) \equiv \int d^3r d^3r' g^{(3)}(\mathbf{r},\mathbf{r}')(1-2\cos(\mathbf{k}\cdot\mathbf{r})+\cos\{[\mathbf{k}\cdot(\mathbf{r}-\mathbf{r}')]\})\times(\mathbf{k}\cdot\boldsymbol{\nabla})(\mathbf{k}\cdot\boldsymbol{\nabla}')(\boldsymbol{\nabla}\cdot\boldsymbol{\nabla}')\beta u(r)\beta u(r'), \tag{A5}$$

by

$$\Delta m^{(3)}(k) = \left[\int d^3r g(r)[1-\cos(\mathbf{k}\cdot\mathbf{r})](\mathbf{k}\cdot\boldsymbol{\nabla})\,\boldsymbol{\nabla}\,\beta u(\mathbf{r})\right]^2. \tag{A6}$$

The corresponding approximate expression for the case of self-diffusion is identical, but without the term involving $\cos(\mathbf{k}\cdot\mathbf{r})$. Thus, within these approximations, the only static input needed by the SCGLE theory is $g(r)$.

APPENDIX B: DERIVATION OF EQ. (2.11)

This appendix summarizes the derivation of Eq. (2.11) provided in detail in Ref. [10]. Consider a monodisperse colloidal suspension formed by N spherical particles in a volume V in the absence of hydrodynamic interactions, whose microscopic dynamics is described by the N-particle Langevin equations [1–3]

$$M\frac{d\mathbf{v}_i(t)}{dt} = -\zeta^o\mathbf{v}_i(t) + \mathbf{f}_i(t) + \sum_{j\neq i}\mathbf{F}_{ij}(t), \quad i=1,2,\ldots,N. \tag{B1}$$

In these equations, M is the mass, $\mathbf{v}_i(t)$ is the velocity, and ζ^o is the free-diffusion friction coefficient, of the ith particle. Also, $\mathbf{f}_i(t)$ is a Gaussian white random force of zero mean, and variance $\langle\mathbf{f}_i(t)\mathbf{f}_j(0)\rangle = k_BT\zeta^o 2\delta(t)\delta_{ij}\,\overleftrightarrow{\mathbf{I}}$ $(i,j=1,2,\ldots,N;$ $\overleftrightarrow{\mathbf{I}}$ being the 3×3 unit tensor). The pairwise force that the jth particle exerts on particle i is given by $\mathbf{F}_{ij}=-\nabla_i u(|\mathbf{r}_i-\mathbf{r}_j|)$.

If one is only interested in the motion of individual tracer particles, then Eq. (B1) for one specific particle (denoted by the index $i=T$) may be rewritten *exactly* as

$$M\frac{d\mathbf{v}_T(t)}{dt} = -\zeta_T^o\mathbf{v}_T(t) + \mathbf{f}_T(t) + \int d^3r[\nabla u(r)]n^*(\mathbf{r},t), \tag{B2}$$

where $n^*(\mathbf{r},t)$ is the local concentration of the other colloidal particles at time t and position $\mathbf{r}$ [referred to the position $\mathbf{x}_T(t)$ of the tracer particle]. In other words, $n^*(\mathbf{r},t)$ is defined as $n^*(\mathbf{r},t)\equiv n[\mathbf{x}_T(t)+\mathbf{r},t]$, with $n(\mathbf{x},t)\equiv\Sigma_{i\neq T}\delta[\mathbf{x}-\mathbf{x}_i(t)]$ being the local concentration at time t and position $\mathbf{x}$, the positions $\mathbf{x}_i(t)$ and $\mathbf{x}$ being referred to the laboratory reference frame.

An important observation is then that the direct interactions between the particles, represented by the pairwise potential $u(r)$, couple *exactly* the motion of the tracer particle with the motion of the other particles *only* through the collective variable $n^*(\mathbf{r},t)$. The equilibrium average $n^{eq}(r)$ of $n^*(\mathbf{r},t)$ is given by $n^{eq}(r)=ng(r)$, with n being the number concentration, and $g(r)$ the radial distribution function of the bulk suspension. Due to the radial symmetry of the force $[-\nabla u(r)]$ and of $n^{eq}(r)$, the integral in Eq. (B2), evaluated at $n^*(\mathbf{r},t)=n^{eq}(r)$, vanishes. Thus, Eq. (B2) is a linear equation coupling exactly the time derivative of the tracer's velocity $\mathbf{v}_T(t)$ with itself and with the variable $\delta n^*(\mathbf{r},t)\equiv n^*(\mathbf{r},t) - n^{eq}(r)$, namely,

$$M\frac{d\mathbf{v}_T(t)}{dt} = -\zeta_T^o\mathbf{v}_T(t) + \mathbf{f}_T(t) + \int d^3r[\nabla u(r)]\delta n^*(\mathbf{r},t). \tag{B3}$$

The variable $\delta n^*(\mathbf{r},t)$ represents the fluctuations around equilibrium of the local concentration of colloidal particles in the presence of the "external" field produced by, and described from a reference frame fixed to, the tracer particle. Thus, we need a relaxation equation that couples the time-derivative of the variable $\delta n^*(\mathbf{r},t)$ with itself and with $\mathbf{v}_T(t)$. Its most general structure is dictated by the general principles of linear irreversible thermodynamics [11] to be a linear version of a generalized diffusion equation, with the following general structure [10]:

$$\frac{\partial\delta n^*(\mathbf{r},t)}{dt} = [\nabla n^{eq}(r)]\cdot\mathbf{v}_T(t) - \int_0^t dt'\int d^3r' D^*(\mathbf{r},\mathbf{r}';t-t') \times\delta n^*(\mathbf{r}',t') + f(\mathbf{r},t), \tag{B4}$$

where the first term on the right-hand side is a linearized streaming term and $f(\mathbf{r},t)$ is a fluctuating term, related to $D^*(\mathbf{r},\mathbf{r}';t)$ by $\int d^3r''\langle f(\mathbf{r},t)f(\mathbf{r}'',t')\rangle\sigma(\mathbf{r}'',\mathbf{r}') = D^*(\mathbf{r},\mathbf{r}';t-t')$, with $\sigma(\mathbf{r},\mathbf{r}')\equiv\langle\delta n^*(\mathbf{r},0)\delta n^*(\mathbf{r}',0)\rangle$.

Formally solving Eq. (B4) and substituting the solution for $\delta n^*(\mathbf{r},t)$ in Eq. (B3) leads to

$$M\frac{d\mathbf{v}_T(t)}{dt} = -\zeta_T^o\mathbf{v}_T(t) + \mathbf{f}_T(t) - \int_0^t dt'\Delta\overleftrightarrow{\zeta}(t-t')\cdot\mathbf{v}_T(t') + \mathbf{F}(t), \tag{B5}$$

where the new fluctuating force $\mathbf{F}(t)$ is related with the time-dependent friction tensor $\Delta\overleftrightarrow{\zeta}(t)$ through $\langle\mathbf{F}(t)\mathbf{F}(0)\rangle = Mk_BT\Delta\overleftrightarrow{\zeta}(t)$, with $\Delta\overleftrightarrow{\zeta}(t)$ given by the following *exact* result:

$$\Delta\overleftrightarrow{\zeta}(t) = -\int d^3r\int d^3r'[\nabla u(r)]\chi^*(\mathbf{r},\mathbf{r}';t)[\nabla' n^{eq}(r')], \tag{B6}$$

where $\chi^*(\mathbf{r},\mathbf{r}';t)$ is the propagator, or Green's function, of the diffusion equation in Eq. (B4), i.e., it solves the equation

$$\frac{\partial\chi^*(\mathbf{r},\mathbf{r}';t)}{dt} = -\int_0^t dt'\int d^3r'' D^*(\mathbf{r},\mathbf{r}'';t-t')\chi^*(\mathbf{r}'',\mathbf{r}';t'), \tag{B7}$$

with initial value $\chi^*(\mathbf{r},\mathbf{r}';t=0)=\delta(\mathbf{r}-\mathbf{r}')$. Notice that, since the initial value $\delta n^*(\mathbf{r},t=0)$ is statistically independent of $\mathbf{v}_T(t)$ and $f(\mathbf{r},t)$, the density-density time-correlation function $G^*(\mathbf{r},\mathbf{r}';t)\equiv\langle\delta n^*(\mathbf{r},t)\delta n^*(\mathbf{r}',0)\rangle$, which is the van Hove function of the particles surrounding the tracer particle, and observed from the tracer particle's reference frame, is also a solution of the same equation with initial value $G^*(\mathbf{r},\mathbf{r}';t=0)=\sigma(\mathbf{r},\mathbf{r}')$.

To simplify the notation, let us rewrite Eq. (B6) as $\Delta\overleftrightarrow{\zeta}(t)=-[\nabla u^\dagger]\circ\chi^*(t)\circ[\nabla n^{eq}]$, where the convolution $\int d^3r''F(\mathbf{r},\mathbf{r}'')G(\mathbf{r}'',\mathbf{r}')$ between two arbitrary functions F and G is written as the matrix product $F\circ G$, and similarly with the "(column) vectors" u and n^{eq}. In this notation, the dagger means transpose. With this notation, let us recall an additional exact relation between the "vectors" u, n^{eq}, and the "matrix" σ. This is the so-called Wertheim-Lovett relation [10,47], $[\nabla n^{eq}]=-\beta\sigma\circ[\nabla u]$, of the equilibrium theory of inhomogeneous fluids. This relation, along with the definition of the inverse matrix σ^{-1}, $[\sigma^{-1}\sigma=I$, with I being the unit

matrix, $I(\mathbf{r},\mathbf{r}')\equiv\delta(\mathbf{r}-\mathbf{r}')$, where δ is Kronecker's Δ function], allows us to write Eq. (B6) in a variety of different but equivalent and exact manners. In particular, we will employ the following:

$$\Delta\overleftrightarrow{\zeta}(t)=k_BT[\nabla n^{eq\dagger}]\circ\sigma^{-1}\circ G^*(t)\circ\sigma^{-1}\circ[\nabla n^{eq}], \quad \text{(B8)}$$

where we have used the fact that the van Hove function $G^*(t)$ can be written as $G^*(t)=\chi^*(t)\sigma$.

This is the exact result for $\Delta\overleftrightarrow{\zeta}(t)$ that leads to the general but approximate expression in Eq. (2.11). The approximations required are related to the general properties of the functions $G^*(\mathbf{r},\mathbf{r}';t)$ and $\sigma(\mathbf{r},\mathbf{r}')$. The latter is just the two-particle distribution function of the colloidal particles surrounding the tracer particle, but subjected to the "external" field $u(r)$ exerted by this tracer particle. Thus, it is effectively a three-particle correlation function. Only if one ignores the effects of such an "external" field, one can write $\sigma(\mathbf{r},\mathbf{r}')=\sigma(|\mathbf{r}-\mathbf{r}'|)\equiv n\delta(\mathbf{r}-\mathbf{r}')+n^2[g(|\mathbf{r}-\mathbf{r}'|)-1]$. Similarly, we may also approximate $G^*(\mathbf{r},\mathbf{r}';t)$ by $G^*(|\mathbf{r}-\mathbf{r}'|;t)$. This is referred to as the "homogeneous fluid approximation" [10], which allows us to write $G^*(\mathbf{r},\mathbf{r}';t)=(1/2\pi)^3\int d^3k\exp[i\mathbf{k}\cdot\mathbf{r}]F^*(k,t)$, with $F^*(k,t)\equiv\langle\Sigma_{i,j}^N\exp\{i\mathbf{k}\cdot[\mathbf{r}_i(t)-\mathbf{r}_j(0)]\}\rangle$. The latter is the intermediate scattering function, except for the asterisk indicating that the position vectors $\mathbf{r}_i(t)$ and $\mathbf{r}_j(0)$ have the origin in the center of the tracer particle. Denoting by $\mathbf{x}_T(t)$ the position of the tracer particle referred to a laboratory-fixed reference frame, we may rewrite $F^*(k,t)\equiv\langle(\exp\{i\mathbf{k}\cdot[\mathbf{x}_T(t)-\mathbf{x}_T(0)]\})\cdot(\Sigma_{i,j}^N\exp\{i\mathbf{k}\cdot[\mathbf{x}_i(t)-\mathbf{x}_j(0)]\})\rangle$, where $\mathbf{r}_i(t)$ is the position of the ith particle in the fixed reference frame. Approximating the average of the product in this expression by the product of the averages, leads to $F^*(k,t)=F(k,t)F_S(k,t)$, which we refer to as the decoupling approximation [10]. The result in Eq. (2.11) is obtained from the exact result in Eq. (B8) above, plus the introduction of the two approximations just described. For spherical particles, the tensor $\Delta\overleftrightarrow{\zeta}(t)$ must be diagonal, $\Delta\overleftrightarrow{\zeta}(t)=\Delta\zeta(t)\,\overleftrightarrow{\mathbf{I}}$, and Eq. (2.11) refers to the scalar function $\Delta\zeta(t)$.

[1] P. N. Pusey, in *Liquids, Freezing and the Glass Transition*, edited by J. P. Hansen, D. Levesque, and J. Zinn-Justin (Elsevier, Amsterdam, 1991).
[2] W. Hess and R. Klein, Adv. Phys. **32**, 173 (1983).
[3] G. Nägele, Phys. Rep. **272**, 215 (1996).
[4] L. Yeomans-Reyna and M. Medina-Noyola, Phys. Rev. E **64**, 066114 (2001).
[5] L. Yeomans-Reyna, H. Acuña-Campa, and M. Medina-Noyola, Phys. Rev. E **62**, 3395 (2000).
[6] L. Yeomans-Reyna and M. Medina-Noyola, Phys. Rev. E **62**, 3382 (2000).
[7] L. Yeomans-Reyna, H. Acuña-Campa, F. de Jesus Guevara-Rodríguez, and M. Medina-Noyola, Phys. Rev. E **67**, 021108 (2003).
[8] M. A. Chávez-Rojo and M. Medina-Noyola, Physica A **366**, 55 (2006).
[9] M. A. Chávez-Rojo and M. Medina-Noyola, Phys. Rev. E **72**, 031107 (2005).
[10] M. Medina-Noyola, Faraday Discuss. Chem. Soc. **83**, 21 (1987).
[11] M. Medina-Noyola and J. L. del Río-Correa, Physica A **146**, 483 (1987).
[12] C. A. Angell, Science **267**, 1924 (1995).
[13] P. G. Debenedetti and F. H. Stillinger, Nature (London) **410**, 359 (2001).
[14] W. Götze, in *Liquids, Freezing and Glass Transition*, edited by J. P. Hansen, D. Levesque, and J. Zinn-Justin (North-Holland, Amsterdam, 1991).
[15] W. Götze and L. Sjögren, Rep. Prog. Phys. **55**, 241 (1992).
[16] W. Götze and E. Leutheusser, Phys. Rev. A **11**, 2173 (1975).
[17] W. Götze, E. Leutheusser, and S. Yip, Phys. Rev. A **23**, 2634 (1981).
[18] W. van Megen and P. N. Pusey, Phys. Rev. A **43**, 5429 (1991).
[19] W. van Megen, S. M. Underwood, and P. N. Pusey, Phys. Rev. Lett. **67**, 1586 (1991).
[20] W. van Megen, T. C. Mortensen, S. R. Williams, and J. Müller, Phys. Rev. E **58**, 6073 (1998).
[21] E. Bartsch *et al.*, J. Chem. Phys. **106**, 3743 (1997).
[22] C. Beck, W. Härtl, and R. Hempelmann, J. Chem. Phys. **111**, 8209 (1999).
[23] G. Szamel and H. Löwen, Phys. Rev. A **44**, 8215 (1991).
[24] N. J. Wagner, Phys. Rev. E **49**, 376 (1994).
[25] (a) G. Nägele, J. Bergenholtz, and J. K. G. Dhont, J. Chem. Phys. **110**, 7037 (1999); (b) **108**, 9893 (1998).
[26] (a) G. Nägele and J. K. G. Dhont, J. Chem. Phys. **108**, 9566 (1998); (b) G. Nägele and P. Baur, Physica A **245**, 297 (1997).
[27] A. J. Banchio, J. Bergenholtz, and G. Nägele, J. Chem. Phys. **113**, 3381 (2000).
[28] A. J. Banchio, J. Bergenholtz, and G. Nägele, Phys. Rev. Lett. **82**, 1792 (1999).
[29] G. Szamel, Phys. Rev. Lett. **90**, 228301 (2003).
[30] J. Wu and J. Cao, Phys. Rev. Lett. **95**, 078301 (2005).
[31] (a) R. Verberg, I. M. de Schepper, and E. G. D. Cohen, Phys. Rev. E **61**, 2967 (2000); (b) E. G. D. Cohen and I. M. de Schepper, J. Stat. Phys. **63**, 242 (1991); (c) I. M. de Schepper, E. G. D. Cohen, P. N. Pusey, and H. N. W. Lekkerkerker, J. Phys.: Condens. Matter **1**, 6503 (1989).
[32] B. Cichocki and B. U. Felderhof, Physica A **204**, 152 (1994).
[33] J. P. Hansen and I. R. McDonald, *Theory of Simple Liquids* (Academic Press, New York, 1976).
[34] J. L. Boon and S. Yip, *Molecular Hydrodynamics* (Dover Publications, New York, 1980).
[35] (a) J. L. Arauz-Lara and M. Medina-Noyola, Physica A **122**, 547 (1983); (b) G. Nägele, M. Medina-Noyola, R. Klein, and J. L. Arauz-Lara, *ibid.* **149**, 123 (1988).
[36] H. Acuña-Campa and M. Medina-Noyola, J. Chem. Phys. **113**, 869 (2000).
[37] G. H. Vineyard, Phys. Rev. **110**, 999 (1958).
[38] J. K. Percus and G. J. Yevick, Phys. Rev. **110**, 1 (1957).
[39] M. S. Wertheim, Phys. Rev. Lett. **10**, 321 (1963).

[40] M. Fuchs, W. Götze, I. Hofacker, and A. Latz, J. Phys.: Condens. Matter **3**, 5047 (1991).
[41] A. J. Banchio, Ph.D. thesis, University of Konstanz, 1999.
[42] F. de J. Guevara-Rodríguez and M. Medina-Noyola, Phys. Rev. E **68**, 011405 (2003).
[43] L. Verlet and J.-J. Weis, Phys. Rev. A **5**, 939 (1972).
[44] E. J. W. Verwey and J. T. G. Overbeck, *Theory of the Stability of Lyophobic Colloids* (Elsevier, Amsterdam, 1948).
[45] M. Medina-Noyola and D. A. McQuarrie, J. Chem. Phys. **73**, 6229 (1980).
[46] F. A. Lindemann, Phys. Z. **11**, 609 (1911).
[47] R. Evans, Adv. Phys. **28**, 143 (1979).
[48] W. Götze and M. R. Mayr, Phys. Rev. E **61**, 587 (2000).
[49] T. Scopigno, G. Ruocco, F. Sette, and G. Monaco, Science **302**, 849 (2003).
[50] U. Buchenau and A. Wischnewski, Phys. Rev. B **70**, 092201 (2004).